Development 139, 3383-3391 (2012) doi:10.1242/dev.081620

Epidermal and cortical roles of *NFP* and *DMI3* in coordinating early steps of nodulation in *Medicago truncatula*

Pauline Rival[1,2], Françoise de Billy[1,2], Jean-Jacques Bono[1,2], Clare Gough[1,2], Charles Rosenberg[1,2,*] and Sandra Bensmihen[1,2,*,‡]

SUMMARY

Legumes have evolved the capacity to form a root nodule symbiosis with soil bacteria called rhizobia. The establishment of this symbiosis involves specific developmental events occurring both in the root epidermis (notably bacterial entry) and at a distance in the underlying root cortical cells (notably cell divisions leading to nodule organogenesis). The processes of bacterial entry and nodule organogenesis are tightly linked and both depend on rhizobial production of lipo-chitooligosaccharide molecules called Nod factors. However, how these events are coordinated remains poorly understood. Here, we have addressed the roles of two key symbiotic genes of *Medicago truncatula*, the lysin motif (LysM) domain-receptor like kinase gene *NFP* and the calcium- and calmodulin-dependent protein kinase gene *DMI3*, in the control of both nodule organogenesis and bacterial entry. By complementing mutant plants with corresponding genes expressed either in the epidermis or in the cortex, we have shown that epidermal *DMI3*, but not *NFP*, is sufficient for infection thread formation in root hairs. Epidermal *NFP* is sufficient to induce cortical cell divisions leading to nodule primordia formation, whereas *DMI3* is required in both cell layers for these processes. Our results therefore suggest that a signal, produced in the epidermis under the control of *NFP* and *DMI3*, is responsible for activating DMI3 in the cortex to trigger nodule organogenesis. We integrate these data to propose a new model for epidermal/cortical crosstalk during early steps of nodulation.

KEY WORDS: *Medicago truncatula*, Root nodule symbiosis, Root epidermis/cortex, Crosstalk, Long distance signalling, LysM-RLK, CCaMK

INTRODUCTION

Legumes can establish a root endosymbiosis with soil bacteria called rhizobia. This association is of great agronomical and ecological interest because the rhizobia can fix atmospheric nitrogen and transfer it to the plant. During establishment of this interaction the plant starts a new developmental programme leading to the formation of a new organ, the root nodule, where the bacteria are hosted. The establishment and maintenance of this symbiosis are dependent on a molecular dialogue between the plant and the bacteria involving the production by rhizobia of lipo-chitooligosaccharide molecules called Nod factors (NFs). NFs are responsible for the induction of early responses in the plant, such as root hair (RH) deformation, calcium oscillations and expression of genes known as early 'nodulin' genes, such as *MtENOD11* (Oldroyd and Downie, 2008). Bacteria then attach to a RH and underlying inner cortical cells are activated by the NF-producing rhizobia to initiate new cell divisions leading to nodule primordium formation (Timmers et al., 1999). Then the RH curls around rhizobia, while the underlying outer cortical cells prepare for bacterial entry by forming so-called pre-infection threads (PITs) (Timmers et al., 1999). Rhizobia enter an RH inside an infection thread (IT) that progresses through the epidermis into the cortex of the root, its direction of growth directed by PITs, until it reaches the dividing inner cortical cells (Timmers et al., 1999).

Thus, infection and nodule development are tightly coupled, although they are initiated in different cell layers of the root. How these two processes are coordinated remains elusive. Forward genetic screens have revealed key players of the NF signalling pathway in the two model plants *Medicago truncatula* and *Lotus japonicus*. In *M. truncatula*, mutants in the *Nod Factor Perception* (*NFP*) gene are the most dramatically impaired for the interaction with the symbiont *Sinorhizobium meliloti*, as they do not nodulate and do not show any symbiotic responses to either rhizobia or purified NFs (Ben Amor et al., 2003). *NFP* encodes a receptor-like kinase with three extracellular lysin motif (LysM) domains and an inactive kinase domain (Arrighi et al., 2006). LysM domains have been shown to bind to N-acetylglucosamine, chitooligosaccharides and peptidoglycan (Kaku et al., 2006; Iizasa et al., 2010; Petutschnig et al., 2010; Willmann et al., 2011) and it is believed that NFP is an NF receptor, although no direct binding of NFs to NFP has been shown. In addition to the complete loss of NF-induced responses in *nfp* mutant roots, knockdown of *NFP* by RNAi and genetic analysis have shown that *NFP* also controls bacterial entry (Arrighi et al., 2006; Bensmihen et al., 2011). Other symbiotic mutants of *M. truncatula* include the *dmi* (*Does not Make Infections*) mutants, which define genes acting downstream of *NFP* in the NF signalling pathway. These mutants are impaired in their interaction with both rhizobia and arbuscular mycorrhizal fungi, and as such the *DMI* genes (*DMI1*, *DMI2* and *DMI3*) control a 'common symbiotic pathway' leading to establishment of both root endosymbioses (Catoira et al., 2000). *DMI1* and *DMI2* are genetically upstream of *DMI3* and are required for DMI3 activation. *DMI3* encodes a calcium- and calmodulin-dependent protein kinase (CCaMK) that is required to 'decipher' the calcium oscillations (known as calcium spiking) triggered by the perception of NFs. *dmi3* mutants show no rhizobial entry, no nodule formation

[1]INRA, Laboratoire des Interactions Plantes-Microorganismes (LIPM), UMR441, F-31326 Castanet-Tolosan, France. [2]CNRS, Laboratoire des Interactions Plantes-Microorganismes (LIPM), UMR2594, F-31326 Castanet-Tolosan, France.

*These authors contributed equally to this work
‡Author for correspondence (sandra.bensmihen@toulouse.inra.fr)

Accepted 21 June 2012

and limited response to NFs. Gain-of-function approaches have shown (both in *M. truncatula* and in *L. japonicus*) that DMI3 controls nodule organogenesis, as autoactive forms of DMI3 can induce the spontaneous formation of nodules in the absence of rhizobia (Gleason et al., 2006; Tirichine et al., 2006). The calmodulin-binding domain of the product of the *L. japonicus* orthologue of *DMI3*, *CCaMK*, is important for rhizobial infection (Shimoda et al., 2012). Moreover, spontaneous nodules formed in *L. japonicus* mutants carrying a constitutively active form of a cytokinin receptor cannot be infected in the absence of *CCaMK* (Hayashi et al., 2010; Madsen et al., 2010). Finally, a *DMI3* gene from rice can complement a *M. truncatula dmi3* mutant for nodule organogenesis, but does not restore normal infection (Godfroy et al., 2006), indicating that legume-specific features of DMI3 are required for rhizobial infection.

Thus, both *NFP* and *DMI3* control rhizobial infection and nodule organogenesis, and *NFP* also controls NF perception. Here, we investigated further the respective roles of *NFP* and *DMI3* in these symbiotic processes in the different cell layers of the root. Although intracellular infection and nodule organogenesis need to be tightly associated for the establishment of the root nodule symbiosis, these two developmental processes can be genetically uncoupled (Oldroyd and Downie, 2008). Therefore, crosstalk between the epidermis and the cortex is necessary for spatially coordinating and synchronising nodule organogenesis with bacterial infection. However, the tissue-specific contributions of players of NF signalling in this crosstalk have never been addressed. Moreover, very little is known about the mechanisms that synchronise cortical cell division (CCD) in the inner cortex and IT formation in overlying RHs.

In this study, we have shown that both *NFP* and *DMI3* are expressed in the epidermis and in the root cortex. Based on this observation, we studied their respective contributions in the control of epidermal and cortical events. To do so, we complemented *nfp* and *dmi3* mutants using tissue-specific expression of *NFP* and *DMI3*, respectively, and looked for the restoration of an early NF signalling event (*MtENOD11* induction), IT formation and nodule organogenesis.

MATERIALS AND METHODS

Plant growth conditions

nfp-2 pMtENOD11:GUS (Arrighi et al., 2006), *dmi3-1* [TRV25 allele, (Lévy et al., 2004)] and *dmi3-1 pMtENOD11:GUS* lines (Catoira et al., 2000) in the *M. truncatula* cv. Jemalong A17 wild-type background were used for all complementation experiments. *pNFP:GUS* stable lines were obtained by transforming *M. truncatula* cv. 2HA by *Agrobacterium tumefaciens* strain AGL1 carrying the pLP100-pNFP:GUS plasmid described by Arrighi et al. (Arrighi et al., 2006). The *pNFP:GUS* expression profile was tested in three independent T3 lines.

Surface-sterilised seeds were sown on agar plates and placed for 3 days in the dark at 4°C then left overnight at 25°C to germinate.

For root transformation, we used ARqua1 *Agrobacterium rhizogenes* as described by Boisson-Dernier et al. (Boisson-Dernier et al., 2001). *A. rhizogenes* transformed roots were selected by *GFP* expression and kanamycin resistance conferred by the pCambia2202 binary vector (http://www.cambia.org/daisy/cambia/585#dsy585_Description).

For nodulation assays, transformed plants were transferred to sepiolite (Agrauxine, Quimper)/sand (2:1 volume mix) pots and grown at 25°C with 18 hour light/6 hour dark cycles (Catoira et al., 2000).

Rhizobial strains and inoculation

Wild-type *S. meliloti* RCR2011 (pXLGD4) (GMI6526) was grown at 28°C in tryptone yeast medium supplemented with 6 mM calcium chloride and 10 μg/ml tetracycline.

The bacteria were ‘scratched’ from the plate after 2 days and resuspended in sterile water. Plants were inoculated twice, at 7 days and 14 days after transfer to pots, with 2 ml of inoculum, adjusted to OD_{600}=0.2, per plant.

Plasmid constructs

All *NFP* cloning was performed using the Multisite Gateway technology (Invitrogen), with BP and LR reactions according to the manufacturer’s instructions. Promoter sequences were introduced in pDONR P4-P1R, NFP coding sequence was reconstructed with the extracellular domain (up to the juxtamembrane domain) in pDONR 221 and the kinase domain in pDONR P2R-P3. All fragments were amplified using either TaKaRa LaTaq (Takara Bio, Japan) or Phusion High Fidelity DNA polymerase (Finnzymes, Finland). All *NFP* amplifications used p2201-NFP (Arrighi et al., 2006) as a template. The *Δgen1-1:GUS* construct described by Bucher et al. (Bucher et al., 2002) was used as a template for pLeEXT1 and the pGII124-PCO2-HYFT construct (kindly provided by R. Heidstra, Department of Molecular Genetics, Utrecht University, Utrecht, The Netherlands) for pCO2. The different PCR fragments were obtained using the primers specified in supplementary material Table S1. Each fragment was subcloned and sequenced in the pGEM-T vector (Promega, USA) and subsequently introduced in the corresponding pDONR vector (Invitrogen) by BP reaction. The three ‘ENTRY clones’ generated in this way were then used for a LR recombination using pAM-pAT-multi as a destination vector [kindly provided by L. Deslandes, Laboratoire des Interactions Plantes Micro-organismes (LIPM), Toulouse, France]. The recombined sequence obtained was then taken out of pAM-pAT-multi by *Asc*I and *Pme*I digestion and subcloned in a pCambia2202 vector, modified for its multiple cloning sites to introduce an *Asc*I site, using the *Asc*I and *Sma*I restrictions sites.

The plasmid containing both the pLeEXT1:NFP and the pCO2:NFP constructs was obtained by ligating two *Asc*I/*Pme*I fragments (containing pLeEXT1:NFP and pCO2:NFP, respectively) in a pCambia2202 vector digested by *Asc*I only.

pCO2 and pLeEXT1 promoters, amplified with pCO2for*Eco*RI/pCO2rev*Kpn*I and pLeEXT1for-*Eco*RI/pLeEXT1rev-*Kpn*I, respectively, were also introduced by a classical (restriction enzyme) cloning method in the *Eco*RI/*Kpn*I sites of pCambia2202, giving the pCambia2202:pLeEXT1 and pCambia2202:pCO2 vectors. NFP versions with these constructs were also generated and gave similar results to the Gateway constructs.

The pDMI3:DMI3 construct (p135H) was described by Lévy et al. (Lévy et al., 2004). To place the cDNA of the full length DMI3 sequence (denoted c-DMI3) under the control of tissue-specific promoters, an *Xba*I/*Sal*I fragment of the plasmid pGreen49:p35S:c-DMI3 (C.R., unpublished data) was introduced in pCambia2202:pLeEXT1 or pCambia2202:pCO2 vectors digested by the same enzyme combination.

For the plasmid containing both pLeEXT1:DMI3 and pCO2:DMI3, a *Xho*I/*Pst*I fragment of the pCO2:DMI3 construct was introduced in the pCambia2202:pLeEXT1-DMI3 vector digested by *Sal*I/*Pst*I.

pCO2:GUS and pDMI3:GUS constructs were obtained by LR recombination in the Gateway destination vector pKGWFS7.0 (Karimi et al., 2002). Promoter sequences were obtained with the attB1for_PCO2/ attB2rev_PCO2 and attBpDMI3F/ attBpDMI3R primers and subcloned by BP reaction in pDONR 221.

pLeEXT1:GUS corresponds to the Δgen1-1:GUS described by Bucher et al. (Bucher et al., 2002) and was kindly provided by M. Bucher to A. Niebel (LIPM, Toulouse, France).

NF treatment

Purified NFs from the *S. meliloti* wild-type strain RCR2011 were provided by F. Maillet (LIPM, Toulouse, France) and used at 10^{-9} M working solution in sterile water.

Transformed roots were transferred to pouch paper/Farhaeus agar plates and incubated for 16 hours in a growth chamber at 25°C with 16 hour light/8 hour dark cycle after either water or NF treatment as described previously (Andriankaja et al., 2007).

Microscopy methods

Histochemical β-glucuronidase (GUS) tests were performed as described previously (Journet et al., 2001). Whole root segments were stained for GUS activity for 3 hours at 37°C with the magenta-glucA (5-bromo-4-chloro-3 indolyl glucuronide, cyclohexylammonium salt) substrate (Duchefa Biochemie, The Netherlands). To visualise bacterial infection, whole roots were fixed under vacuum for 15 minutes with 1.5% glutaraldehyde phosphate-buffered solution followed by one hour fixation in the same solution. Histochemical staining of β-galactosidase activity expressed by the plasmid pXLGD4 was performed as described previously (Ardourel et al., 1994). Whole root segments were observed with a Leica MZFLIII stereomicroscope (Leica Microsystems, Wetzlar, Germany).

For further analysis, 70 μm- or 50 μm-thick and 5 μm-thick sections were made using a vibratome (Leica VT1000S) or a microcut (2040 Reichert Jung), respectively. Fragments were embedded in 4% agarose solution for the 70 μm- or 50 μm-thick sections and in Technovit 7100 resin (Heraeus Kulzer, Wehrheim, Germany) for the 5 μm sections. Observations were performed on a Zeiss Axioplan2 imaging microscope.

Statistical analyses

Non-parametric Kruskal-Wallis tests were performed using the Statgraphics Centurion software (Sigma Plus).

RESULTS

NFP and *DMI3* are expressed both in the epidermis and in the cortex of the root during nodulation

The *NFP* expression pattern in *Medicago truncatula* was previously reported using *Agrobacterium rhizogenes* transformed roots (Arrighi et al., 2006), but no root sections were performed. To analyse this expression pattern further, we generated stable pNFP:GUS plant lines and made sections on both non-inoculated roots and roots inoculated with *Sinorhizobium meliloti*. In young non-inoculated roots, pNFP:GUS expression was strong (Fig. 1A) and we observed pNFP:GUS expression in the epidermis, as previously shown (Arrighi et al., 2006), but also in cortical layers (Fig. 1A). Upon inoculation at 4 days post inoculation (dpi), pNFP:GUS was strongly and locally expressed in cortical cells underlying IT progression and before any nodule 'outgrowth' could be observed (Fig. 1B) but was weaker in the epidermis, as previously shown by Arrighi et al. (Arrighi et al., 2006). Subsequent pNFP:GUS expression was also observed, as previously shown (Arrighi et al., 2006), in the infection zone of mature nodules 10 dpi (data not shown).

The *DMI3* tissue expression pattern in *M. truncatula* has so far been described only in RHs (Smit et al., 2005) and nodules (Limpens et al., 2005) but no other root cell layer or spatiotemporal expression data during nodulation are available. Thus, we introduced a pDMI3:GUS construct in wild-type roots by *A. rhizogenes* transformation and looked for its tissue expression pattern in non-inoculated roots and upon infection with *S. meliloti*. Whereas in non-inoculated roots (Fig. 1C) *GUS* expression was faint in the epidermis and in the cortex, it increased upon inoculation at 2 dpi, especially in RH cells (Fig. 1D). During infection, pDMI3:GUS expression was stronger in cortical cells where ITs progressed and in the underlying layers in front of ITs (Fig. 1E). In young nodules, pDMI3:GUS activity was detected in the whole nodule cortex (data not shown). In mature nodules, pDMI3:GUS was expressed in the infection zone at 12 dpi (Fig. 1F), as shown by Limpens and colleagues using in situ hybridisation (Limpens et al., 2005).

Thus, before and during early steps of the *M. truncatula/S. meliloti* symbiosis, both *DMI3* and *NFP* were found to be expressed in the epidermis and in the cortex and both were upregulated in dividing cortical cells, ahead of IT progression. To understand their respective contributions to the establishment of symbiosis in the root epidermis and in the root cortex, we decided to complement mutant plants by expressing *DMI3* or *NFP* specifically either in the epidermis or in the cortex.

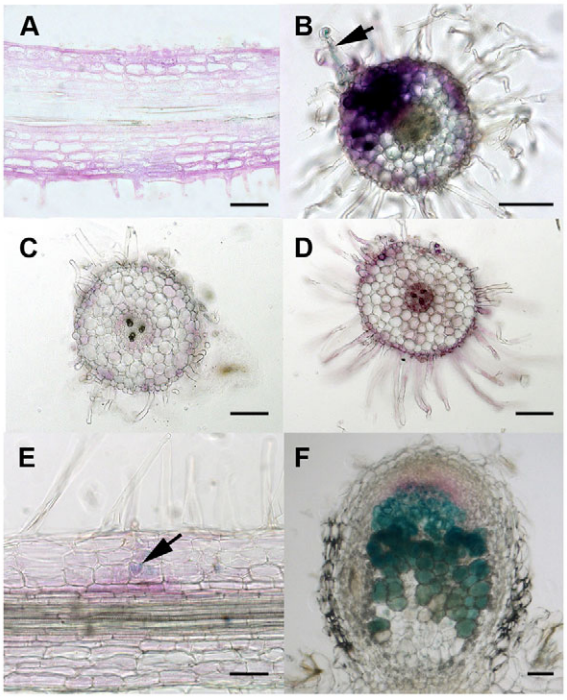

Fig. 1. Expression patterns of *NFP* and *DMI3* promoter GUS fusions in *M. truncatula* non-inoculated roots and upon inoculation with *S. meliloti*. (**A**) Longitudinal section of a non-inoculated pNFP:GUS root showing expression in both the epidermis and the cortex. (**B**) Transverse section showing that pNFP:GUS expression is highly induced in nodule primordia (4 dpi) opposite IT progression (arrow). (**C**) Root section from pDMI3:GUS non-inoculated roots. (**D**) pDMI3:GUS expression is enhanced in RHs and the cortex, 2 dpi with *S. meliloti*. (**E**) pDMI3:GUS expression upon rhizobia infection, 4 dpi. A progressing IT is shown by an arrow. (**F**) pDMI3:GUS expression in the infection zone of an elongated nodule, 12 dpi with *S. meliloti*. For roots transformed with the pDMI3:GUS construct, six to 13 independent plants were sectioned for each time point and representative profiles are shown. For pNFP:GUS, stable transgenic plants were used. GUS activity is shown in magenta; β-galactosidase activity revealing bacterial presence is shown in blue in B, E and F. A is a 5 μm-thick section, B-F are 50 μm-thick sections. Scale bars: 100 μm.

pLeEXT1 and pCO2 as tissue-specific promoters in *M. truncatula* roots

We chose pLeEXT1 for epidermal expression. This promoter, originally described in tomato (Bucher et al., 2002), was shown to be expressed specifically in *M. truncatula* RH cells (Mirabella et al., 2004). Using a pLeEXT1:GUS construct, we checked for this tissue-specific expression, before and after *S. meliloti* inoculation. In non-inoculated plants, the observation of whole roots and root sections revealed that pLeEXT1 was active in RH and non-RH epidermal cells whereas no expression could be detected in the root cortex (Fig. 2A,C). The expression of pLeEXT1:GUS decreased in mature RHs and was absent in older parts of main roots, as described by Mirabella et al. (Mirabella et al., 2004) (Fig. 2E). pLeEXT1:GUS was thus expressed in the 'NF susceptible zone'

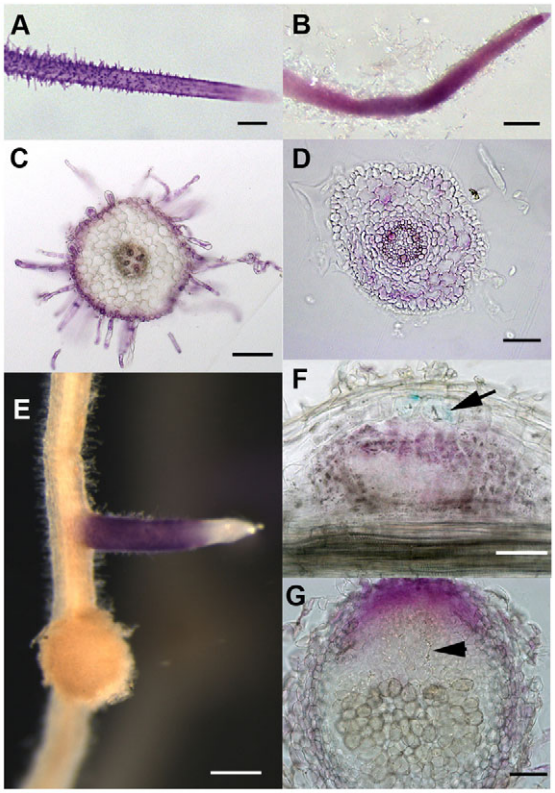

Fig. 2. Expression patterns of pLeEXT1 and pCO2 promoter GUS fusions in *M. truncatula* wild-type non-inoculated roots and upon inoculation with *S. meliloti*. (**A**) pLeEXT1:GUS and (**B**) pCO2:GUS in non-inoculated whole roots. (**C**,**D**) Transverse non-inoculated root sections showing expression of pLeEXT1:GUS in the root epidermis, but no detectable expression in the cortex (C) and expression of pCO2:GUS in the root cortex but not in the epidermis (D). (**E**) pLeEXT1:GUS in transformed wild-type root, 7 dpi with *S. meliloti*, showing expression in a young lateral root but not in a nodule. (**F**) pCO2:GUS activity is clearly detected inside a young bump (dividing cortical cells) (4 dpi) prior to infection (a progressing IT is shown by an arrow) but is still absent from the epidermis. (**G**) Nodule section at 10 dpi showing strong pCO2:GUS activity in the nodule apex. An IT is shown by an arrow. GUS activity is shown in magenta; β-galactosidase activity revealing bacterial presence is shown in blue in F. D is a 5 μm-thick section, C, F and G are 50 μm-thick sections. Scale bars: 1 mm in A,B,E; 100 μm in C,D,F,G.

where the plant can perceive rhizobia (Bhuvaneswari et al., 1981). Upon *S. meliloti* inoculation, epidermal expression of pLeEXT1:GUS was unchanged in young roots and was absent from nodules, consistent with the fact that nodules do not have an epidermal cell layer (Fig. 2E) (data not shown).

For cortical expression, we used pCO2 from *Arabidopsis* (Heidstra et al., 2004). To our knowledge, this promoter had not been tested in *Medicago* and we checked its expression using a pCO2-driven GUS reporter gene (Fig. 2). In non-inoculated roots (Fig. 2B), pCO2:GUS was absent from the root epidermis and present throughout the cortex, as shown by cross-sections (Fig. 2D). During nodulation, GUS expression was detected in the dividing cells of the root cortex forming young nodules (Fig. 2F). In more mature nodules (10 dpi), GUS expression was clearly visible in the apex of nodules adjacent to the infection zone (Fig. 2G).

To check further the validity of both promoters for our tissue-specific complementation assays, we took advantage of a very sensitive reporter gene, *pMtENOD11:GUS*, which is only expressed in the epidermis in response to purified NFs (Charron et al., 2004; Journet et al., 2001). As NFP is a presumptive NF receptor, we used pLeEXT1:NFP and pCO2:NFP to complement *nfp pMtENOD11:GUS* mutant plants and looked for the ability of each construct to restore *pMtENOD11:GUS* activity upon application of purified NFs. As shown in Fig. 3, pLeEXT1:NFP (Fig. 3C, n=26/54), but not pCO2:NFP (Fig. 3B, n=0/26), could complement for *pMtENOD11:GUS* expression upon NF application at 10^{-9} M, as did the pNFP:NFP construct (Fig. 3D, n=26/45). This indicates that pLeEXT1:NFP is correctly expressed in the epidermis to allow NF perception. By contrast, the absence of *pMtENOD11:GUS* induction by the pCO2:NFP construct strongly indicates that there is no *NFP* expression in the epidermis, or that it is not sufficient to lead to *pMtENOD11:GUS* expression.

Therefore, the use of the pLeEXT1 and pCO2 promoters seemed appropriate, as they were able to restrict the expression of a reporter gene in the specific cell types.

Epidermal expression of *DMI3* can rescue bacterial infection whereas epidermal expression of *NFP* rescues nodule organogenesis

Next, we tested the ability of the pLeEXT1:NFP and pLeEXT1:DMI3 constructs to complement *nfp pMtENOD11:GUS* and *dmi3 pMtENOD11:GUS* plants, respectively. We examined plants at 7 dpi and 21 dpi both for infection (i.e. presence of ITs) and for different steps of nodule organogenesis [initial CCDs leading to visible bumps, small round nodules and pink (functional) elongated nodules]. We also analysed *pMtENOD11:GUS* expression in inoculated plants because *pMtENOD11:GUS* is also expressed in response to bacterial infection. Indeed, Journet et al. have shown that the expression of *pMtENOD11:GUS* is widespread along the root epidermis in response to NF-producing rhizobia whereas it becomes restricted to infection sites when the bacteria start entering RHs. Later on, *pMtENOD11:GUS* expression

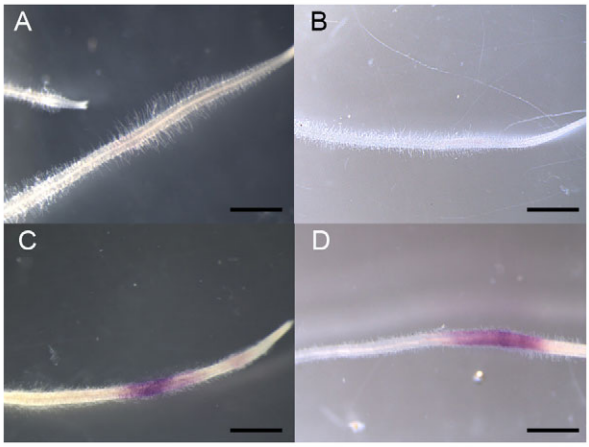

Fig. 3. Induction of *pMtENOD11:GUS* expression in pCO2:NFP-, pLeEXT1:NFP- or pNFP:NFP-transformed *nfp pMtENOD11:GUS* roots by pure Nod Factor treatment. (**A-D**) *nfp pMtENOD11:GUS* roots were transformed by an empty vector (A), pCO2:NFP (B), pLeEXT1:NFP (C) or pNFP:NFP (D) and treated with 10^{-9} M purified NF from *S. meliloti* for 16 hours. GUS activity is shown in magenta. Scale bars: 1 mm.

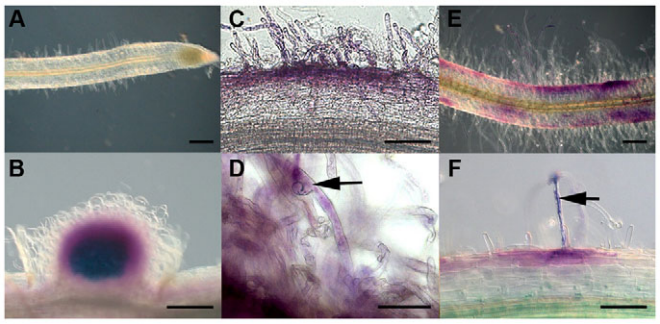

Fig. 4. Complementation of *nfp* and *dmi3 pMtENOD11:GUS* plants by the pLeEXT1:NFP and pLeEXT1:DMI3 constructs at 7 dpi with *S. meliloti*. (**A**) *dmi3 pMtENOD11:GUS* root transformed by an empty vector. (**B**) *dmi3 pMtENOD11:GUS* root transformed by a pDMI3:DMI3 construct showing a young infected nodule. (**C**) Longitudinal section of *nfp pMtENOD11:GUS* root transformed with the pLeEXT1:NFP construct showing strong epidermal *pMtENOD11:GUS* expression but (**D**) only bacteria entrapped in curled RH (arrow) and no ITs. (**E**) *dmi3 pMtENOD11:GUS* root transformed with the pLeEXT1:DMI3 construct showing *pMtENOD11:GUS* expression. (**F**) *dmi3 pMtENOD11:GUS* root transformed with the pLeEXT1:DMI3 construct showing IT formation in an RH (arrow). GUS activity is shown in magenta; β-galactosidase activity revealing bacterial presence is shown in blue in B, D and F. C is an 80 μm-thick section. Scale bars: 100 μm.

is also associated with nodule organogenesis in the root cortex (Journet et al., 2001).

Whereas *nfp* and *dmi3* mutants were completely deficient for infection, cell division and *pMtENOD11:GUS* expression at any time after inoculation (Fig. 4A, Fig. 5A), as previously described (Ben Amor et al., 2003; Catoira et al., 2000), the pNFP:NFP *nfp* or pDMI3:DMI3 *dmi3* control plants showed young nodule formation by 7 dpi (Fig. 4B). In the case of *nfp pMtENOD11:GUS* roots complemented by pLeEXT1:NFP, strong epidermal *pMtENOD11:GUS* expression could be seen at 7 dpi (Fig. 4C), but rhizobia were only rarely entrapped in curled RHs, and, neither IT initiation nor CCD could be observed (Fig. 4C,D). By contrast, both *pMtENOD11:GUS* expression (Fig. 4E) and frequent IT formation in RHs (Fig. 4F, Table 1) were observed with the pLeEXT1:DMI3 construct in *dmi3 pMtENOD11:GUS* roots at 7 dpi, but no CCD was observed (Fig. 4F).

At 21 dpi, whereas the control pNFP:NFP and pDMI3:DMI3 constructs led to good nodule organogenesis and infection in their corresponding mutant backgrounds (Fig. 5B, Fig. 6), pLeEXT1:NFP *nfp* plants mainly showed bumps with typical *pMtENOD11:GUS* expression (forming in 53/59 plants) (Fig. 6A) and bacteria were entrapped in RHs but ITs were still absent (Fig. 5C). In pLeEXT1:DMI3 *dmi3* plants, IT formation was frequently observed but no CCD was ever seen opposite the ITs (36 plants) (Fig. 5D, Fig. 6B). These ITs progressed within the epidermal cell but were blocked at the junction with the cortical cell (Fig. 5D). Therefore, epidermal *NFP* could trigger nodule organogenesis but no IT formation, whereas epidermal *DMI3* did not restore nodule organogenesis but could restore IT formation restricted to the epidermis.

No significant complementation for nodulation, infection or *pMtENOD11:GUS* expression of the mutant phenotypes was observed with the pCO2:NFP (n=59) or pCO2:DMI3 (n=18) constructs (Fig. 6) (data not shown). Therefore, we investigated whether expression of either gene simultaneously under both the epidermal and the cortical promoters (i.e. pLeEXT1+pCO2) could improve the restoration of infection and nodule organogenesis.

Combining epidermal and cortical expression restores nodule organogenesis for DMI3

Constructs consisting of pLeEXT1:NFP and pCO2:NFP, or pLeEXT1:DMI3 and pCO2:DMI3 cloned on the same plasmid were introduced in *A. rhizogenes* for complementation studies in *nfp* or *dmi3* mutants.

In the case of *NFP*, at 7 dpi, the pLeEXT1:NFP+pCO2:NFP construct did not significantly improve complementation compared with the pLeEXT1-driven version alone. Thus, the pLeEXT1:NFP+pCO2:NFP construct did not restore infection in *nfp* plants as bacteria were still only entrapped in curled RHs and

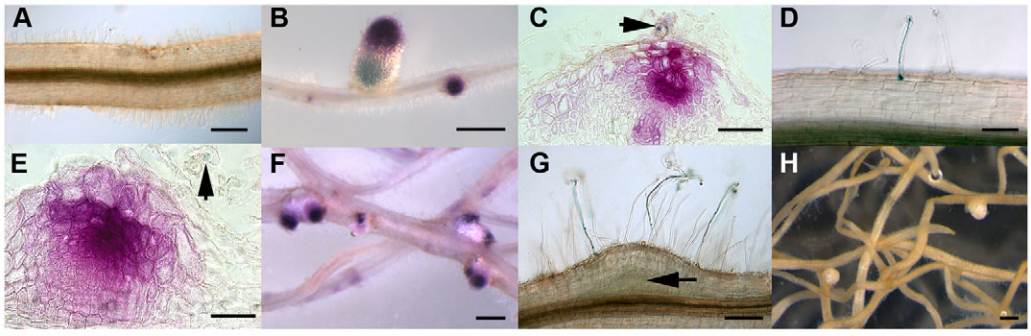

Fig. 5. Complementation of *nfp pMtENOD11:GUS* and *dmi3* plants by the pLeEXT1:NFP and pLeEXT1:DMI3, or the pLeEXT1:NFP+pCO2:NFP and pLeEXT1:DMI3+pCO2:DMI3 constructs at 21 dpi with *S. meliloti*. (**A**) *nfp pMtENOD11:GUS* root transformed by an empty vector. (**B**) *nfp pMtENOD11:GUS* root transformed by the pNFP:NFP construct, showing infected nodules. (**C**) *nfp pMtENOD11:GUS* root transformed by the pLeEXT1:NFP construct, showing a bump with bacteria entrapped in a curled RH (arrow). (**D**) *dmi3* root transformed by the pLeEXT1:DMI3 construct showing an IT in an RH. (**E**) Section of a bump obtained with the pLeEXT1:NFP+pCO2:NFP construct in *nfp pMtENOD11:GUS* roots did not show any infection and bacteria remained entrapped in a curled RH (arrow). (**F**) *nfp pMtENOD11:GUS* roots transformed with the pLeEXT1:NFP+pCO2:NFP construct, showing uninfected nodules. (**G**) *dmi3* (not transgenic for *pMtENOD11:GUS*) root transformed by the pLeEXT1:DMI3+pCO2:DMI3 construct showing IT progression in RHs only and activation of CCD opposite the ITs (arrow). (**H**) *dmi3* (not transgenic for *pMtENOD11:GUS*) root transformed by the pLeEXT1:DMI3+pCO2:DMI3 construct, showing uninfected nodules. GUS activity is shown in magenta; β-galactosidase activity revealing bacterial presence is shown in blue in B-E and G. C and E are 5 μm-thick sections. Scale bars: 1 mm in A,B,F,H; 50 μm in E; 100 μm in C,D,G.

Table 1. Quantification of infection thread formation in root hairs in *dmi3 pMtENOD11:GUS* plants complemented by the pDMI3:DMI3, pLeEXT1:DMI3 or pLeEXT1:DMI3+pCO2:DMI3 constructs at 7 dpi with *S. meliloti*

	Constructs		
	pDMI3:DMI3	pLeEXT1:DMI3	pLeEXT1:DMI3 +pCO2:DMI3
Infection threads/cm (mean)	3.7[a]	13.5[b]	8.1[c]
Number of roots	37	91	75

Results are averages of three experiments.
[a,b,c]Statistically different means, as shown by Student's t-test (P<0.001).

no ITs could be seen (data not shown). In the later stages, at 21 dpi, the pLeEXT1:NFP+pCO2:NFP *nfp* plants showed CCD leading to bump formation together with *pMtENOD11:GUS* expression typical of young nodules (Fig. 5E, on 43/46 plants, Fig. 6A). More uninfected nodules (Fig. 5F) were observed than with the pLeEXT1:NFP construct: on 12/46 plants for the pLeEXT1:NFP+pCO2:NFP construct versus 12/59 plants for the pLeEXT1:NFP construct, with an average of 1.5 versus 0.54 per plant (Fig. 6A). However, no IT formation could be detected associated with these structures or with the bumps (Fig. 5E).

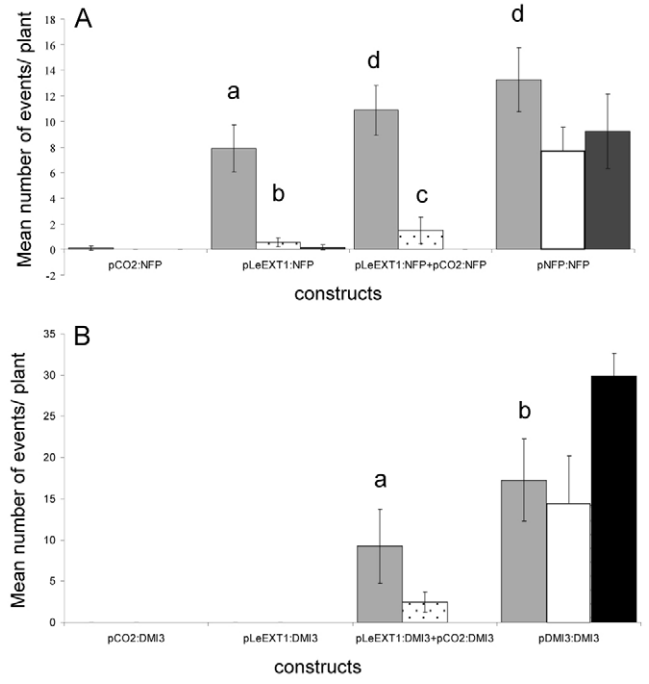

Fig. 6. Quantification of the different nodule organogenesis structures observed in *nfp* and *dmi3* roots transformed with the different tissue-specific constructs at 21 dpi with *S. meliloti*. The mean number of each type of structure was calculated for: bumps (grey bars), small uninfected nodules (dotted bars), small infected and uninfected nodules (white bars) and pink elongated nodules (black bars) observed at 21 dpi with *S. meliloti*. (**A**) *nfp* mutant roots transformed by the pCO2:NFP, pLeEXT1:NFP, pLeEXT1:NFP+pCO2:NFP or pNFP:NFP constructs, on 46-59 transformed plants (per construct) from two independent experiments. (**B**) *dmi3* mutant roots transformed by the pCO2:DMI3, pLeEXT1:DMI3, pLeEXT1:DMI3+pCO2:DMI3 or pDMI3:DMI3 constructs, on 34-36 transformed plants (per construct) from three independent experiments. Error bars represent the 95% confidence interval. Statistical difference of the means (inside the same structure category) was assessed by a Kruskal-Wallis (non parametric) test, the different categories discriminated by this test (with P<0.01) are shown by lower-case letters.

For *DMI3*, the pLeEXT1:DMI3+pCO2:DMI3 construct could restore CCD opposite ITs (11/23 plants, Fig. 5G) as soon as 7 dpi in *dmi3* plants, which was never observed with pLeEXT1:DMI3 or pCO2:DMI3 alone (n=30 and n=23, respectively). Moreover, IT numbers, although still higher than with pDMI3:DMI3, were reduced compared with complementation with pLeEXT1:DMI3, indicating partial restoration of the control of infection events (Table 1). At later stages (21 dpi), bumps and uninfected nodules were also formed (Fig. 5H, in 14/36 plants, Fig. 6B). However, no progression of ITs into the cortex (Fig. 5G) was observed.

Thus, compared with expression restricted just to the epidermis, the additional expression of *DMI3* in the cortex allowed CCD and nodule organogenesis to proceed and restored some negative feedback on epidermal IT formation. For *NFP*, nodule organogenesis, already observed with the pLeEXT1:NFP construct, was significantly improved with the pLeEXT1:NFP+pCO2:NFP construct. However, in both cases, the use of the pLeEXT1+pCO2 constructs did not restore the progression of infection in the *nfp* and *dmi3* mutants.

DISCUSSION

The coordinated control of rhizobial infection and nodule organogenesis leading to successful establishment of root nodule symbiosis is poorly understood. Previous data have shown that the cortex prepares for IT progression [with PITs (Timmers et al., 1999) and calcium spiking (Sieberer et al., 2012)] and it has been proposed that secondary signalling transmits information from the site of bacterial entry in RHs to trigger cell divisions within the cortex for nodule organogenesis (for a review, see Oldroyd et al., 2011). However, no studies have uncoupled the respective contributions of these two cell layers. Here, we have used tissue-specific promoters to drive the expression of *NFP* and *DMI3* either in the epidermis or in the cortex to uncouple their epidermal and cortical contributions to the control of rhizobial infection and nodule organogenesis.

NFP and *DMI3* are expressed in both the epidermis and the cortex

NFP and *DMI3* were fused to the GUS reporter gene to analyse their spatiotemporal expression patterns during early symbiotic steps. For both pNFP:GUS and pDMI3:GUS, we detected constitutive expression (prior to rhizobial inoculation) that was uniform in the root epidermis and in the root cortex. This is compatible with very early symbiotic roles of *NFP* and *DMI3*. Upon rhizobial inoculation, pNFP:GUS expression was quickly and strongly upregulated and became restricted to cortical cells underlying ITs growing in RHs. pDMI3:GUS expression was first upregulated in RHs, prior to IT formation (at 2 dpi), and then in cortical cells underlying or containing ITs. For both promoters, the enhanced expression levels appeared to precede actual infection and CCD, suggesting that these genes control early steps of both processes and have important

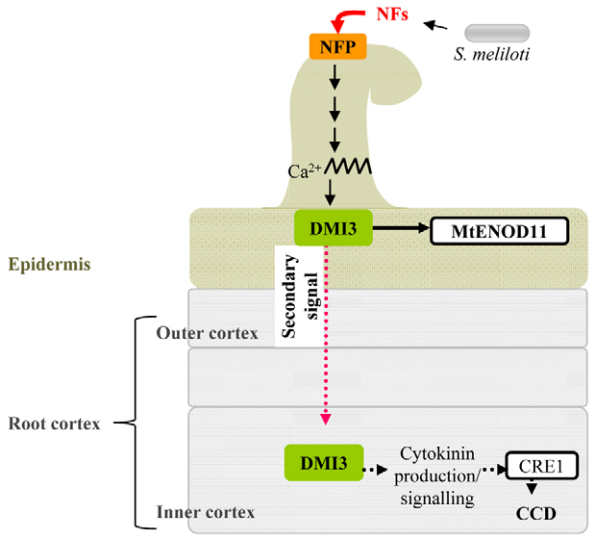

Fig. 7. Model for the control of nodule organogenesis by NFP and DMI3. Cortical cell division (CCD) can be triggered through a signalling cascade that is activated by NFP and DMI3 in the epidermis. This involves calcium spiking and leads to the activation of *MtENOD11* expression in the epidermis. The nature of the secondary signal is unknown and is unlikely to be cytokinins but would lead to the activation of DMI3 in the cortex. In turn, cortical DMI3 would activate the cytokinin production/signalling pathway (via the cytokinin receptor CRE1) leading to CCD and nodule organogenesis.

symbiotic roles not only in the epidermis for initial NF perception, but also in the cortex for subsequent steps.

pLeEXT1 and pCO2 are useful promoters for tissue-specific complementation approaches in *M. truncatula*

As described by Mirabella et al. (Mirabella et al., 2004), we demonstrated that the tomato promoter pLeEXT1 has good root epidermis specificity in *M. truncatula*. Moreover, the pLeEXT1:GUS epidermal pattern and its absence of expression in the cortex were conserved during nodulation. Furthermore, pLeEXT1:NFP could complement *nfp* mutants for the well-characterised epidermal NF-specific response that is the induction of *pMtENOD11:GUS*. pCO2:GUS activity was detected in all cortical layers of the root, but not in epidermal cells. Upon nodulation, pCO2 activity was also clearly restricted to internal parts of the root, notably dividing cortical cells. Furthermore, the fact that no CCD and no *pMtENOD11:GUS* activity could be observed with pCO2:NFP or pCO2:DMI3 alone in the corresponding mutant backgrounds showed that pCO2 activity in the epidermis of *M. truncatula* roots was either absent or too weak to allow any induction of these symbiotic responses.

Taken together, these data support the suitability of pLeEXT1 and pCO2 promoters for tissue-specific complementation approaches during symbiotic events in *M. truncatula*.

Nodule organogenesis is controlled by epidermal *NFP* and by both epidermal and cortical *DMI3*

Our observation that restricting *NFP* expression to the epidermis was sufficient to induce nodule organogenesis suggests that *NFP* acts in a non-cell-autonomous manner to trigger cell divisions in the cortex. Because multiple cell layers separate the site of initial bacterial contact at the RH surface from the site of cell division in the inner cortex, the role of a secondary signal has been suggested for the induction of these cell divisions (Oldroyd et al., 2011). Our observation that epidermal *NFP* expression is sufficient to induce nodule organogenesis supports this hypothesis. NFP would thus be required to perceive NFs in the epidermis and generate this secondary signal, but would not be necessary in inner tissues for induction of CCD and nodule organogenesis (Fig. 7).

Unlike *NFP*, epidermal *DMI3* expression was not sufficient to restore induction of CCD. No CCDs were observed either in *dmi3* mutants complemented by the pCO2:DMI3 construct, showing that cortical expression of *DMI3* is not sufficient. By contrast, when the *dmi3* mutant was complemented by the double construct with both promoters, cell divisions occurred in the inner cortex leading to the formation of small, uninfected nodules. These results show that the induction of CCD requires expression of *DMI3* both in the epidermis and in the cortex (Fig. 7). Although the key role of DMI3 in controlling CCD has already been demonstrated using gain-of-function alleles (Gleason et al., 2006; Tirichine et al., 2006), no data has so far shown the need for DMI3 in the cortex. If nodule organogenesis requires secondary signalling between the epidermis and the cortex, our results indicate that DMI3 is involved at two different levels in this signalling mechanism. This CCaMK would thus be required in the epidermis for the generation of a secondary signal in response to NFs, and in the cortex for the perception/transduction of this secondary signal (Fig. 7).

Epidermis-cortex signalling leading to nodule organogenesis

The nature of the signal generated by epidermal NF perception and which would trigger the organogenesis programme in the root cortex is not known, but the hormones cytokinin and abscisic acid are possible candidates as they are involved in nodule organogenesis (Ding and Oldroyd, 2009; Frugier et al., 2008; Oldroyd and Downie, 2008). In *L. japonicus*, genetic studies have shown that the cytokinin receptor gene *LHK1* acts downstream of *CCaMK* (Hayashi et al., 2010; Heckmann et al., 2011; Tirichine et al., 2007). Taken together, we propose that cortical DMI3 acts upstream of cytokinin perception to activate nodule organogenesis (Fig. 7) and that cytokinin is probably not the secondary signal generated in the epidermis as DMI3 would not be necessary in the cortex in this case (Fig. 7). This is consistent with reports showing that cytokinin signalling is restricted to cortical cells (Oldroyd et al., 2011; Plet et al., 2011).

Some authors have suggested that this secondary signal could involve GRAS or 'Notch-like' transcription factor movement (Hirsch and Oldroyd, 2009; Oldroyd and Downie, 2008). However, as these transcription factors are genetically downstream of *DMI3* both for epidermal and cortical responses (Gleason et al., 2006; Marsh et al., 2007), this hypothesis is not compatible with the need for DMI3 in the cortex. Calcium is also an interesting candidate, but *L. japonicus* mutants with a very low epidermal calcium-spiking response can induce cortical responses leading to nodule organogenesis (Groth et al., 2010; Kosuta et al., 2011). If calcium is not itself the secondary signal, the need for a CCaMK in the cortex strongly suggests that the signalling pathway activated in the cortex involves a calcium signal. New players such as nitric oxide could also play a role in different steps of symbiosis establishment (for a review, see Meilhoc et al., 2011).

Epidermal expression of *DMI3*, but not of *NFP*, is sufficient for root hair infection

nfp and *dmi3* mutant complementation by epidermal-driven genes led to striking differences in the infection process, from which we

can conclude that NFP and DMI3 play distinct roles in the control of IT initiation and progression. In *dmi3* plants complemented by pLeEXT1:DMI3, ITs were initiated and developed normally inside RHs. This showed an important role for epidermal *DMI3* in IT formation, and is consistent with data obtained in *L. japonicus* in which epidermal infection of spontaneous nodules (obtained by activation of the cytokinin receptor LHK1) is not possible in a *ccamk* mutant background (Hayashi et al., 2010; Madsen et al., 2010). Furthermore, the fact that in *dmi3* pLeEXT1:DMI3 plants ITs aborted when they reached the apposed cortical cell (where *DMI3* was not expressed) indicates that *DMI3* acts in a cell-autonomous manner to control IT formation. The absence of IT progression in the cortex is consistent with recent data showing that high frequency calcium oscillations occur in the outer cortical cell that will be infected, but not in the neighbouring cells (Sieberer et al., 2012). Taken together, these data suggest an involvement of *DMI3* in the cortical infection process. Moreover, the leucine-rich repeat receptor-like protein kinase (LRR-RLK) MtDMI2, which is implicated in activating the CCaMK (Hayashi et al., 2010), is expressed in the cortex during nodule development (Bersoult et al., 2005).

In *nfp* mutant plants complemented by pLeEXT1:NFP, bacteria could be entrapped in curled RHs, but no ITs were observed. It is unlikely that the expression of *NFP* under the pLeEXT1 promoter is incompatible with restoration of infection in RHs because wild-type plants expressing pLeEXT1:NFP are not impaired for nodulation (J. Cullimore, personal communication). The strong activity of the native *NFP* promoter in cortical cells ahead of and during infection (Fig. 1B) (Arrighi et al., 2006) is consistent with a need for NFP in the cortex, possibly to control PIT formation, which is tightly coupled with early steps of infection (Timmers et al., 1999). Therefore *NFP* could control IT formation in a non-cell-autonomous manner, which would be independent of the presence of DMI3 in the cortex.

Because we did not obtain infected nodules when either *NFP* or *DMI3* expression was restricted to the epidermis or to the cortex, and given the fact that both *DMI3* and *NFP* are expressed in both tissues when driven by their own promoters, we tested whether the simultaneous expression of these genes in both tissues could restore infection to mutant plants. The constructs combining the pLeEXT1 and pCO2 promoters were functional for nodule organogenesis, as shown by the restoration of nodule formation in *dmi3* plants and increased nodule organogenesis in *nfp* plants. Also, in these complemented *dmi3* plants, there were significantly fewer ITs in RHs compared with *dmi3* pLeEXT1:DMI3 plants. This suggests a negative control from dividing cortical cells on the number of epidermal infection events, as described for cytokinin receptor mutants (Gonzalez-Rizzo et al., 2006; Murray et al., 2007).

Full infection was not restored in either mutant by these double constructs. An explanation for this could be that infection requires a strict control of the timing and/or level of expression of *NFP* and *DMI3* between the epidermis and the cortex. Nevertheless, full complementation with formation of infected functional nodules can be obtained when *NFP* or *DMI3* expression is driven by the CaMV 35S promoter (data not shown), which has been shown to be strongly and constitutively expressed in most root tissues (Auriac and Timmers, 2007). An alternative hypothesis is that in the pLeEXT1+pCO2 double constructs, cortical expression of *NFP* and *DMI3* driven by the pCO2 promoter, though functional for nodule organogenesis and the control of the number of infection events, does not reach the critical level required in sub-epidermal outer cortical cells for infection to proceed. This is supported by the observation that IT progression in outer cortical cells during early steps of nodulation is associated with a lower level of pCO2:GUS activity compared with the inner dividing cortical cells (Fig. 2F). Also, the pNFP:GUS and pDMI3:GUS constructs show increased GUS expression associated with infection (Fig. 1B,E) (Arrighi et al., 2006), suggesting that *NFP* and *DMI3* have to be expressed more highly for cortical cells to become infected. However, as we cannot completely rule out other explanations, such as a need for these genes to be expressed in other tissues, we cannot formally conclude that cortical expression of *NFP* and *DMI3* is required for the infection process.

Concluding remarks

In this work we have shown that *NFP* and *DMI3*, through non-cell-autonomous or cell-autonomous functions, control spatial crosstalks between the epidermis and the cortex during establishment of nodulation. We have also highlighted different mechanisms underlying infection and nodule organogenesis, and provided more data concerning the coordination of these symbiotic processes. LYK3 is another putative NF receptor that is expressed in both the epidermis and the cortex of *M. truncatula* roots (Haney et al., 2011; Mbengue et al., 2010), and *lyk3* mutants are defective in both PIT formation and infection (Catoira et al., 2001). Hence, LYK3 is also likely to play a role in coordinating the infection process in both cell layers.

The approach that we used to uncouple the contributions of NFP and DMI3 in two different cell layers of the root was a tissue-specific complementation approach of symbiotic mutants. This type of approach could be extended in *M. truncatula* and other legume species by the discovery of endogenous tissue-specific promoters, using tissue-specific transcriptomics, for example. Such promoters should also be useful to study the involvement of different cell layers in other plant/microbe interactions.

Acknowledgements
We thank S. Rivas and J. Cullimore for critical reading of the manuscript.

Funding
P.R. was supported by a fellowship from the French Ministry of Research and Education. This work was funded by the French Agence Nationale de la Recherche [contract ANR-05-BLAN-0243-01 'NodBindsLysM'] and by the European Community's Sixth Framework Programme through a Marie Curie Research Training Network [contract MRTN-CT-2006-035546 'NODPERCEPTION']. This work was supported by funds from the 'Laboratoire d'Excellence (LABEX)' entitled TULIP [ANR-10-LABX-41].

Competing interests statement
The authors declare no competing financial interests.

Supplementary material
Supplementary material available online at
http://dev.biologists.org/lookup/suppl/doi:10.1242/dev.081620/-/DC1

References

Andriankaja, A., Boisson-Dernier, A., Frances, L., Sauviac, L., Jauneau, A., Barker, D. G. and de Carvalho-Niebel, F. (2007). AP2-ERF transcription factors mediate Nod factor dependent Mt ENOD11 activation in root hairs via a novel cis-regulatory motif. *Plant Cell* **19**, 2866-2885.

Ardourel, M., Demont, N., Debellé, F., Maillet, F., de Billy, F., Promé, J. C., Dénarié, J. and Truchet, G. (1994). Rhizobium meliloti lipooligosaccharide nodulation factors: different structural requirements for bacterial entry into target root hair cells and induction of plant symbiotic developmental responses. *Plant Cell* **6**, 1357-1374.

Arrighi, J. F., Barre, A., Ben Amor, B., Bersoult, A., Soriano, L. C., Mirabella, R., de Carvalho-Niebel, F., Journet, E. P., Ghérardi, M., Huguet, T. et al. (2006). The Medicago truncatula lysine motif-receptor-like kinase gene family includes NFP and new nodule-expressed genes. *Plant Physiol.* **142**, 265-279.

Auriac, M. C. and Timmers, A. C. (2007). Nodulation studies in the model legume Medicago truncatula: advantages of using the constitutive EF1alpha

promoter and limitations in detecting fluorescent reporter proteins in nodule tissues. *Mol. Plant Microbe Interact.* **20**, 1040-1047.
Ben Amor, B., Shaw, S. L., Oldroyd, G. E., Maillet, F., Penmetsa, R. V., Cook, D., Long, S. R., Dénarié, J. and Gough, C. (2003). The NFP locus of Medicago truncatula controls an early step of Nod factor signal transduction upstream of a rapid calcium flux and root hair deformation. *Plant J.* **34**, 495-506.
Bensmihen, S., de Billy, F. and Gough, C. (2011). Contribution of NFP LysM domains to the recognition of Nod factors during the Medicago truncatula/Sinorhizobium meliloti symbiosis. *PLoS ONE* **6**, e26114.
Bersoult, A., Camut, S., Perhald, A., Kereszt, A., Kiss, G. B. and Cullimore, J. V. (2005). Expression of the Medicago truncatula DM12 gene suggests roles of the symbiotic nodulation receptor kinase in nodules and during early nodule development. *Mol. Plant Microbe Interact.* **18**, 869-876.
Bhuvaneswari, T. V., Bhagwat, A. A. and Bauer, W. D. (1981). Transient susceptibility of root cells in four common legumes to nodulation by rhizobia 10.1104/pp.68.5.1144. *Plant Physiol.* **68**, 1144-1149.
Boisson-Dernier, A., Chabaud, M., Garcia, F., Bécard, G., Rosenberg, C. and Barker, D. G. (2001). Agrobacterium rhizogenes-transformed roots of Medicago truncatula for the study of nitrogen-fixing and endomycorrhizal symbiotic associations. *Mol. Plant Microbe Interact.* **14**, 695-700.
Bucher, M., Brunner, S., Zimmermann, P., Zardi, G. I., Amrhein, N., Willmitzer, L. and Riesmeier, J. W. (2002). The expression of an extensin-like protein correlates with cellular tip growth in tomato. *Plant Physiol.* **128**, 911-923.
Catoira, R., Galera, C., de Billy, F., Penmetsa, R. V., Journet, E. P., Maillet, F., Rosenberg, C., Cook, D., Gough, C. and Dénarié, J. (2000). Four genes of Medicago truncatula controlling components of a nod factor transduction pathway. *Plant Cell* **12**, 1647-1666.
Catoira, R., Timmers, A. C., Maillet, F., Galera, C., Penmetsa, R. V., Cook, D., Dénarié, J. and Gough, C. (2001). The HCL gene of Medicago truncatula controls Rhizobium-induced root hair curling. *Development* **128**, 1507-1518.
Charron, D., Pingret, J. L., Chabaud, M., Journet, E. P. and Barker, D. G. (2004). Pharmacological evidence that multiple phospholipid signaling pathways link Rhizobium nodulation factor perception in Medicago truncatula root hairs to intracellular responses, including Ca2+ spiking and specific ENOD gene expression. *Plant Physiol.* **136**, 3582-3593.
Ding, Y. and Oldroyd, G. E. (2009). Positioning the nodule, the hormone dictum. *Plant Signal. Behav.* **4**, 89-93.
Frugier, F., Kosuta, S., Murray, J. D., Crespi, M. and Szczyglowski, K. (2008). Cytokinin: secret agent of symbiosis. *Trends Plant Sci.* **13**, 115-120.
Gleason, C., Chaudhuri, S., Yang, T., Muñoz, A., Poovaiah, B. W. and Oldroyd, G. E. (2006). Nodulation independent of rhizobia induced by a calcium-activated kinase lacking autoinhibition. *Nature* **441**, 1149-1152.
Godfroy, O., Debellé, F., Timmers, T. and Rosenberg, C. (2006). A rice calcium- and calmodulin-dependent protein kinase restores nodulation to a legume mutant. *Mol. Plant Microbe Interact.* **19**, 495-501.
Gonzalez-Rizzo, S., Crespi, M. and Frugier, F. (2006). The Medicago truncatula CRE1 cytokinin receptor regulates lateral root development and early symbiotic interaction with Sinorhizobium meliloti. *Plant Cell* **18**, 2680-2693.
Groth, M., Takeda, N., Perry, J., Uchida, H., Dräxl, S., Brachmann, A., Sato, S., Tabata, S., Kawaguchi, M., Wang, T. L. et al. (2010). NENA, a Lotus japonicus homolog of Sec13, is required for rhizodermal infection by arbuscular mycorrhiza fungi and rhizobia but dispensable for cortical endosymbiotic development. *Plant Cell* **22**, 2509-2526.
Haney, C. H., Riely, B. K., Tricoli, D. M., Cook, D. R., Ehrhardt, D. W. and Long, S. R. (2011). Symbiotic rhizobia bacteria trigger a change in localization and dynamics of the Medicago truncatula receptor kinase LYK3. *Plant Cell* **23**, 2774-2787.
Hayashi, T., Banba, M., Shimoda, Y., Kouchi, H., Hayashi, M. and Imaizumi-Anraku, H. (2010). A dominant function of CCaMK in intracellular accommodation of bacterial and fungal endosymbionts. *Plant J.* **63**, 141-154.
Heckmann, A. B., Sandal, N., Bek, A. S., Madsen, L. H., Jurkiewicz, A., Nielsen, M. W., Tirichine, L. and Stougaard, J. (2011). Cytokinin induction of root nodule primordia in Lotus japonicus is regulated by a mechanism operating in the root cortex. *Mol. Plant Microbe Interact.* **24**, 1385-1395.
Heidstra, R., Welch, D. and Scheres, B. (2004). Mosaic analyses using marked activation and deletion clones dissect Arabidopsis SCARECROW action in asymmetric cell division. *Genes Dev.* **18**, 1964-1969.
Hirsch, S. and Oldroyd, G. E. (2009). GRAS-domain transcription factors that regulate plant development. *Plant Signal. Behav.* **4**, 698-700.
Iizasa, E., Mitsutomi, M. and Nagano, Y. (2010). Direct binding of a plant LysM receptor-like kinase, LysM RLK1/CERK1, to chitin in vitro. *J. Biol. Chem.* **285**, 2996-3004.
Journet, E. P., El-Gachtouli, N., Vernoud, V., de Billy, F., Pichon, M., Dedieu, A., Arnould, C., Morandi, D., Barker, D. G. and Gianinazzi-Pearson, V. (2001). Medicago truncatula ENOD11: a novel RPRP-encoding early nodulin gene expressed during mycorrhization in arbuscule-containing cells. *Mol. Plant Microbe Interact.* **14**, 737-748.
Kaku, H., Nishizawa, Y., Ishii-Minami, N., Akimoto-Tomiyama, C., Dohmae, N., Takio, K., Minami, E. and Shibuya, N. (2006). Plant cells recognize chitin fragments for defense signaling through a plasma membrane receptor. *Proc. Natl. Acad. Sci. USA* **103**, 11086-11091.
Karimi, M., Inzé, D. and Depicker, A. (2002). GATEWAY vectors for Agrobacterium-mediated plant transformation. *Trends Plant Sci.* **7**, 193-195.
Kosuta, S., Held, M., Hossain, M. S., Morieri, G., Macgillivary, A., Johansen, C., Antolín-Llovera, M., Parniske, M., Oldroyd, G. E., Downie, A. J. et al. (2011). Lotus japonicus symRK-14 uncouples the cortical and epidermal symbiotic program. *Plant J.* **67**, 929-940.
Lévy, J., Bres, C., Geurts, R., Chalhoub, B., Kulikova, O., Duc, G., Journet, E. P., Ané, J. M., Lauber, E., Bisseling, T. et al. (2004). A putative Ca2+ and calmodulin-dependent protein kinase required for bacterial and fungal symbioses. *Science* **303**, 1361-1364.
Limpens, E., Mirabella, R., Fedorova, E., Franken, C., Franssen, H., Bisseling, T. and Geurts, R. (2005). Formation of organelle-like N2-fixing symbiosomes in legume root nodules is controlled by DMI2. *Proc. Natl. Acad. Sci. USA* **102**, 10375-10380.
Madsen, L. H., Tirichine, L., Jurkiewicz, A., Sullivan, J. T., Heckmann, A. B., Bek, A. S., Ronson, C. W., James, E. K. and Stougaard, J. (2010). The molecular network governing nodule organogenesis and infection in the model legume Lotus japonicus. *Nat. Commun.* **1**, 10.
Marsh, J. F., Rakocevic, A., Mitra, R. M., Brocard, L., Sun, J., Eschstruth, A., Long, S. R., Schultze, M., Ratet, P. and Oldroyd, G. E. (2007). Medicago truncatula NIN is essential for rhizobial-independent nodule organogenesis induced by autoactive calcium/calmodulin-dependent protein kinase. *Plant Physiol.* **144**, 324-335.
Mbengue, M., Camut, S., de Carvalho-Niebel, F., Deslandes, L., Froidure, S., Klaus-Heisen, D., Moreau, S., Rivas, S., Timmers, T., Hervé, C. et al. (2010). The Medicago truncatula E3 ubiquitin ligase PUB1 interacts with the LYK3 symbiotic receptor and negatively regulates infection and nodulation. *Plant Cell* **22**, 3474-3488.
Meilhoc, E., Boscari, A., Bruand, C., Puppo, A. and Brouquisse, R. (2011). Nitric oxide in legume-rhizobium symbiosis. *Plant Sci.* **181**, 573-581.
Mirabella, R., Franken, C., van der Krogt, G. N., Bisseling, T. and Geurts, R. (2004). Use of the fluorescent timer DsRED-E5 as reporter to monitor dynamics of gene activity in plants. *Plant Physiol.* **135**, 1879-1887.
Murray, J. D., Karas, B. J., Sato, S., Tabata, S., Amyot, L. and Szczyglowski, K. (2007). A cytokinin perception mutant colonized by Rhizobium in the absence of nodule organogenesis. *Science* **315**, 101-104.
Oldroyd, G. E. and Downie, J. A. (2008). Coordinating nodule morphogenesis with rhizobial infection in legumes. *Annu. Rev. Plant Biol.* **59**, 519-546.
Oldroyd, G. E., Murray, J. D., Poole, P. S. and Downie, J. A. (2011). The rules of engagement in the legume-rhizobial symbiosis. *Annu. Rev. Genet.* **45**, 119-144.
Petutschnig, E. K., Jones, A. M. E., Serazetdinova, L., Lipka, U. and Lipka, V. (2010). The lysin motif receptor-like kinase (LysM-RLK) CERK1 is a major chitin-binding protein in Arabidopsis thaliana and subject to chitin-induced phosphorylation. *J. Biol. Chem.* **285**, 28902-28911.
Plet, J., Wasson, A., Ariel, F., Le Signor, C., Baker, D., Mathesius, U., Crespi, M. and Frugier, F. (2011). MtCRE1-dependent cytokinin signaling integrates bacterial and plant cues to coordinate symbiotic nodule organogenesis in Medicago truncatula. *Plant J.* **65**, 622-633.
Shimoda, Y., Han, L., Yamazaki, T., Suzuki, R., Hayashi, H. and Imaizumi-Anraku, H. (2012). Rhizobial and fungal symbioses show different requirements for calmodulin binding to calcium calmodulin-dependent protein kinase in *Lotus japonicus*. *Plant Cell* **24**, 304-321.
Sieberer, B. J., Chabaud, M., Fournier, J., Timmers, A. C. J. and Barker, D. G. (2012). A switch in Ca2+ spiking signature is concomitant with endosymbiotic microbe entry into cortical root cells of Medicago truncatula. *Plant J.* **69**, 822-830.
Smit, P., Raedts, J., Portyanko, V., Debellé, F., Gough, C., Bisseling, T. and Geurts, R. (2005). NSP1 of the GRAS protein family is essential for rhizobial Nod factor-induced transcription. *Science* **308**, 1789-1791.
Timmers, A. C., Auriac, M. C. and Truchet, G. (1999). Refined analysis of early symbiotic steps of the Rhizobium-Medicago interaction in relationship with microtubular cytoskeleton rearrangements. *Development* **126**, 3617-3628.
Tirichine, L., Imaizumi-Anraku, H., Yoshida, S., Murakami, Y., Madsen, L. H., Miwa, H., Nakagawa, T., Sandal, N., Albrektsen, A. S., Kawaguchi, M. et al. (2006). Deregulation of a Ca2+/calmodulin-dependent kinase leads to spontaneous nodule development. *Nature* **441**, 1153-1156.
Tirichine, L., Sandal, N., Madsen, L. H., Radutoiu, S., Albrektsen, A. S., Sato, S., Asamizu, E., Tabata, S. and Stougaard, J. (2007). A gain-of-function mutation in a cytokinin receptor triggers spontaneous root nodule organogenesis. *Science* **315**, 104-107.
Willmann, R., Lajunen, H. M., Erbs, G., Newman, M. A., Kolb, D., Tsuda, K., Katagiri, F., Fliegmann, J., Bono, J. J., Cullimore, J. V. et al. (2011). Arabidopsis lysin-motif proteins LYM1 LYM3 CERK1 mediate bacterial peptidoglycan sensing and immunity to bacterial infection. *Proc. Natl. Acad. Sci. USA* **108**, 19824-19829.